

1 **A GIS tool for automatic calculation of glacier equilibrium-line altitudes.**

2 **Ramón Pellitero^{*1}, Brice R. Rea², Matteo Spagnolo³, Jostein Bakke⁴, Susan Ivy-Ochs⁵, Philip**
3 **Hughes⁶, Sven Lukas⁷, Adriano Ribolini⁸.**

4 ¹. Department of Geography and Environment. University of Aberdeen. St Mary's, Elphinstone Road.
5 AB24 3UF Aberdeen (United Kingdom). r.pellitero-ondicol@abdn.ac.uk

6 * Corresponding author

7 ². Department of Geography and Environment. University of Aberdeen. St Mary's, Elphinstone Road.
8 AB24 3UF Aberdeen (United Kingdom). b.rea@abdn.ac.uk

9 ³. Department of Geography and Environment. University of Aberdeen. St Mary's, Elphinstone Road.
10 AB24 3UF Aberdeen (United Kingdom). m.spagnolo@abdn.ac.uk

11 ⁴. Department of Earth Science. University of Bergen, P.O.Box 7800 5020 Bergen (Norway).
12 Jostein.Bakke@geog.uib.no

13 ⁵. Insitut für Teilchenphysik, ETH-Höggerberg. Otto-Stern-Weg 5, 8093 Zürich Switzerland.
14 ivy@phys.ethz.ch

15 ⁶. Geography, School of Environment, Education and Development, University of Manchester, Oxford
16 Road, Manchester M13 9PL (United Kingdom). Philip.Hughes@manchester.ac.uk

17 ⁷. School of Geography, Queen Mary, University of London. Mile End Road London E1 4NS (United
18 Kingdom). s.lukas@qmul.ac.uk

19 ⁸. Dipartimento Scienze della Terra - Università di Pisa - Via S. Maria 53 - 56126
20 Pisa. ribolini@dst.unipi.it

21 **Abstract:**

22 A toolbox for the automated calculation of glacier **equilibrium-line altitudes** (ELAs) using the
23 Accumulation Area Ratio, Accumulation Area Balance Ratio, Altitude Area and Kurowski methods is
24 presented. These are the most commonly-used methods of ELA calculation in palaeo-glacier
25 reconstructions. The toolbox has been coded in Python and runs in ArcGIS requiring only the
26 reconstructed surface of the palaeo-glacier (a DEM) as input. Through fast and automatic calculation
27 this toolbox simplifies the process of palaeo-ELA determination and can successfully work both for a
28 single glacier and for large datasets of multiple glaciers.

29 **Keywords**

30 Equilibrium-line altitude, glacier, GIS, Accumulation Area Ratio, Accumulation Area Balance Ratio,
31 Python

32 **1. Introduction**

33 The Equilibrium Line Altitude (ELA) is the average elevation where, over a one-year time interval,
34 accumulation equals ablation so the mass balance at this line is zero (Cogley et al., 2011). The ELA is

35 significant for the understanding of both present-day and past climates and changes in ELA elevation
36 can be used to track changes in climate. It is important to note that palaeoglacier reconstructions
37 determine the ELA assuming the glacier is in equilibrium with climate. This is equivalent to the zero
38 net balance ELA for extant glaciers, whereas annually the ELA can be highly variable. The ELA is
39 coupled with the climate mainly through **winter precipitation**, which correlates with accumulation
40 (although this also is impacted by windblown snow accumulation and avalanching), and **summer air**
41 **temperature**, which correlates with ablation (although other factors such as incoming shortwave
42 and longwave radiation, sensible heat fluxes and snowpack warming from refreezing can play a
43 significant role). To a first order variations in the ELA are commonly attributed to changes in one or
44 both of these climatic variables. Relationships have been established between precipitation and
45 temperature at the ELA (Ahlmann, 1924; 1948; Krenke and Khodakov, 1966; Loewe, 1971;
46 Braithwaite, 1985; Ohmura et al., 1992; Braithwaite, 2008) which makes it possible to determine one
47 of the two parameters provided the other (usually the temperature) is known. Palaeoglacier
48 reconstructions can therefore yield a quantitative measure of palaeo-precipitation which is difficult
49 to determine using other palaeoclimate proxies.

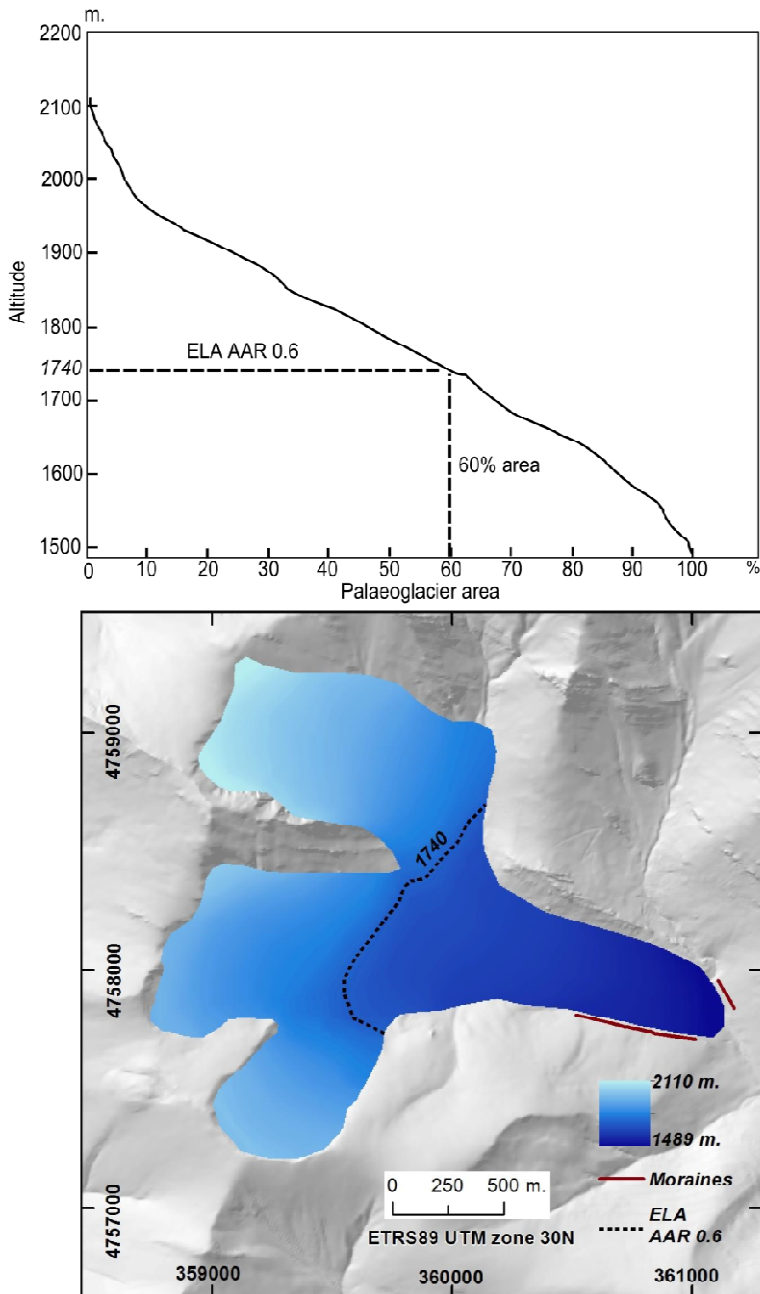
50 Palaeoclimatic reconstructions based on former glacier geometries typically make use of the
51 calculated ELA and its relationship with palaeo-precipitation and palaeo-temperature (Bakke et al.,
52 2005; Benn and Ballantyne, 2005; Lukas and Bradwell, 2010; Hughes et al., 2010). ELAs have also
53 been used to assess the ablation and accumulation in areas where glaciers currently exist but where
54 no climatic data is available (Hughes et al., 2009a).

55 **2. Methods for ELA calculation**

56 **MELM, CFA and HM** - Various methods have been developed and applied to calculate palaeoglacier
57 ELAs. These can be divided into two groups; those which are solely based on the position (specifically
58 the elevation) of glacial landforms and those which also require the geometry of the reconstructed
59 palaeoglacier surface. Examples of the former are the Maximum Elevation of Lateral Moraines
60 (MELM; Lichtnecker, 1938), Cirque Floor Altitudes (CFA; Pewé and Reger, 1972) or the concentration
61 of land-surface area (Hypsometric Maxima, HM; Egholm et al., 2009). These are theoretically correct
62 ELA estimates, but they suffer from potentially significant errors. For example: CFA is only applicable
63 to specific types of glaciers which have formed over multiple glaciations, and the hypsometric
64 maxima are dependent on the dynamics of the glacier and the geological history of the area where
65 the glacier develops (Barr and Spagnolo, 2014). These shortcomings make landform-based ELA
66 estimates useful for first-order (and rapid in the case of MELM and CFA) estimates, but ideally
67 palaeoclimatic reconstructions should not be made based on these palaeo-ELAs. More reliable
68 methods require the part or all of the reconstructed geometry of the palaeoglacier, derived from the
69 position of glacial landforms and the palaeoglacier bed topography; examples of these are the Toe to
70 Headwall Altitude Ratio (THAR), the Accumulation Area Ratio (AAR), the Median Glacier Elevation
71 (MGE or Kurowski) and the Accumulation Area Balance Ratio (AABR).

72 **THAR** - The THAR assumes that the ELA lies at some fixed proportion of the vertical distance (i.e.
73 altitudinal range) between the lowest and highest point of the palaeoglacier, usually in the range
74 0.35-0.5. It can provide a rapid and simple method for a first approximation of the ELA, but it may
75 have large errors when the glacier geometry is complex (Benn and Lehmkuhl, 2000) and is only
76 suitable for topographically constrained glaciers.

77 **AAR** - The AAR is the most widely applied technique for ELA estimation, and it has been used for
78 glacier-climate reconstructions in mountain ranges across the world (e.g. Kerschner et al., 2000,
79 Porter, 2001, Benn and Ballantyne, 2005, Lukas, 2007; Stansell et al., 2007, Pellitero, 2013). The AAR
80 method assumes that the ratio between the accumulation area and the ablation area is constant if
81 glaciers are in steady state (Figure 1). However, this ratio does not take into account the mass
82 balance gradient, which critically is controlled, to the first order, by the regional climate and further
83 modified by local topoclimatic conditions. The mass balance gradient is a proxy for overall ice flux
84 and it is typically steeper (higher accumulation and higher ablation) on warm, wet, maritime glaciers
85 and shallower for cold, dry polar and continental glaciers. The AAR method also fails to account for
86 the hypsometry, i.e. the area-altitude distribution of the reconstructed glacier surface (Osmaston,
87 2005).



88

89 Figure 1. Visualisation of the ELA AAR applied to the Valdenievas palaeoglacier in N Spain, with an
 90 AAR of 0.6. (a) Shows the altitude range plotted against the cumulative percentage area of the
 91 glacier surface. (b) Shows the reconstructed palaeoglacier area and the contour corresponding to
 92 the ELA (Pellitero 2012).

93 The main input needed for calculation of the AAR is the reconstructed 3D glacier-surface. The planar
 94 surface area is sometimes used (Rea et al., 1999), although it can be significantly less accurate. 3D
 95 ice surface reconstructions are normally derived by either interpolation and extrapolation of
 96 mapped glacier limits (i.e. freehand drawing of glacier margins and surface contours onto a base
 97 map) here referred to as the cartographic method (e.g. Ballantyne, 1989; Benn and Ballantyne, 2005;

98 Lukas and Bradwell, 2010) or from numerical reconstructions based on glacier physics (e.g. Rea and
 99 Evans, 2007; Benn and Hulton, 2010).

100 Knowledge of mass-balance gradients is not required for the AAR method but the ratio of the
 101 accumulation area to total area for the reconstructed glacier is. This ratio should ideally be
 102 determined from measurements of extant, similar glaciers in the region (Benn and Lehmkuhl, 2000),
 103 but this is often impossible where glaciers no longer exist. Hughes et al. (2007) and Hughes et al.
 104 (2010) attempted to get around this issue for palaeoglaciers in Greece and Montenegro by applying
 105 a range of AARs to populations of reconstructed glaciers following Osmaston (2002). This involves
 106 taking the altitudes corresponding to 11 evenly-spaced accumulation area ratios of between 0 and 1
 107 (0, 0.1, 0.2, 0.3, 0.4, 0.5, 0.6, 0.7, 0.8, 0.9, 1.0). The standard deviation of each AAR for the group of
 108 glaciers was calculated and the AAR with the lowest standard deviation was chosen. Various authors
 109 have suggested different ratios depending on the type, size and location of glaciers (Table 1).

Paper	Type of glacier (Location)	Ratio
Bakke and Nesje (2011)	Cirque and valley	0.6 ±0.05
Ignéczi and Nagy (2013)	Outlet	0.58
(Gross et al., 1978)	Cirque, valley and icefields (Alps)	0.67
Braithwaite and Müller (1980)	(Arctic, Alpine and Asian)	0.67
	(North America and Scandinavia)	0.5
	(Extremely high relief areas such as Andes or Himalayas)	<0.5
Clark et al. (1994)	Debris covered glaciers	0.2-0.1
Kern and Lazlo (2010)	0.1-1 km ² extension	0.44 ±0.07
	1-4 km ² extension	0.54±0.07
	Larger than 4 km ²	0.64 ± 0.04
	All glaciers (World Glacier Inventory)	0.559 ± 0.09
Leonard (1984), Hughes et al. (2010)	Ice caps	Up to 0.8

110 Table 1. AAR ratios suggested in the scientific literature.

111 **Kurowski or MGE** - An alternative and simpler method to the AAR is that proposed by Kurowski
 112 (1891). This is based on the assumption that, for a glacier in equilibrium where mass balance is a
 113 linear function of altitude, the ELA is situated at the mean glacier elevation (Braithwaite and Raper,
 114 2007). The Kurowski method was adopted by Drygalski (1942) but then fell out of use (Osmaston,
 115 2005). However, it became re-established during the 1960s and 1970s when it was applied by
 116 Osmaston (1965, 1975) working in East Africa and later for reconstructing Loch Lomond Stadial
 117 (Younger Dryas) glaciers in Great Britain (Sissons 1979; Gray, 1982; Sutherland, 1984; Ballantyne,
 118 1989; Hughes, 2002, 2009b). For a glacier with a symmetrical distribution of area with altitude the
 119 mean elevation is approximately equal to the median elevation of the glacier, which is equivalent to
 120 an AAR of 0.5 (Braithwaite and Raper, 2007). The median glacier elevation has been used in the
 121 World Glacier Inventory since the late 1970s (Müller et al., 1977; despite being mistakenly called the
 122 “mean” in Müller et al., 1977; an error corrected in Braithwaite and Müller, 1980). Braithwaite and
 123 Raper (2007, 2009) found a very high correlation (0.998) between the ELA and MGE, based on a
 124 dataset of 144 glaciers with mass balance records of ≥5 years.

125 **AABR (and AA)** - The second-most widely used ELA calculation technique is the AABR method
 126 (Osmaston, 1975; Furbish and Andrews, 1984). This is recognized to be more robust than the AAR

127 and MGE methods because it takes into account both the glacier hypsometry (Osmaston, 2005) and
 128 the mass balance gradients (Benn and Lehmkuhl, 2000). The AABR method is based on three
 129 assumptions: (a) the accumulation and ablation gradients are approximately linear; (b) the net ratio
 130 between ablation and accumulation is known and remains fixed through time (Benn and Lehmkuhl
 131 2000; Rea, 2009); and (c) the topography is assumed to constrain the glacier, so a change in climate
 132 (mass balance) is reflected in a change in the elevation of the terminus. This is not the case for
 133 piedmont glaciers that extend onto lowland plains. This method also recognizes that any given unit
 134 area of the glacier surface that is altitudinally further away from the ELA (either positive or negative)
 135 has a greater contribution to overall mass balance than a unit area that is located closer to the ELA.
 136 The AABR method is best suited to snow-fed, clean glaciers, and strictly speaking should not be
 137 applied to: glaciers that receive a significant mass inputs from avalanching; glaciers where either, or
 138 both, mass balance gradients are not linear; glaciers where extensive debris cover exerts a strong
 139 influence on the ablation gradient (Benn and Lehmkuhl, 2000; Osmaston, 2005). These criteria can
 140 be assessed where there is an extant glacier but are essentially impossible to ascertain for
 141 palaeoglaciers. The AABR method requires the glacier hypsometry and the Balance Ratio (BR). The
 142 latter is a crucial element of the AABR method, as it accounts for the differences between the
 143 accumulation and ablation gradients and their respective contribution to the glacier mass balance. It
 144 can be calculated from the glacier hypsometry using the following (Furbish and Andrews 1894)
 145 (Equation 2):

$$BR = \frac{\bar{Z}_{ac}A_{ac}}{\bar{Z}_{ab}A_{ab}}$$

146 Where:

147 \bar{Z}_{ac} = Area-weighted mean altitude of the accumulation area.

148 A_{ac} = Area of accumulation.

149 \bar{Z}_{ab} = Area-weighted mean altitude of the ablation area.

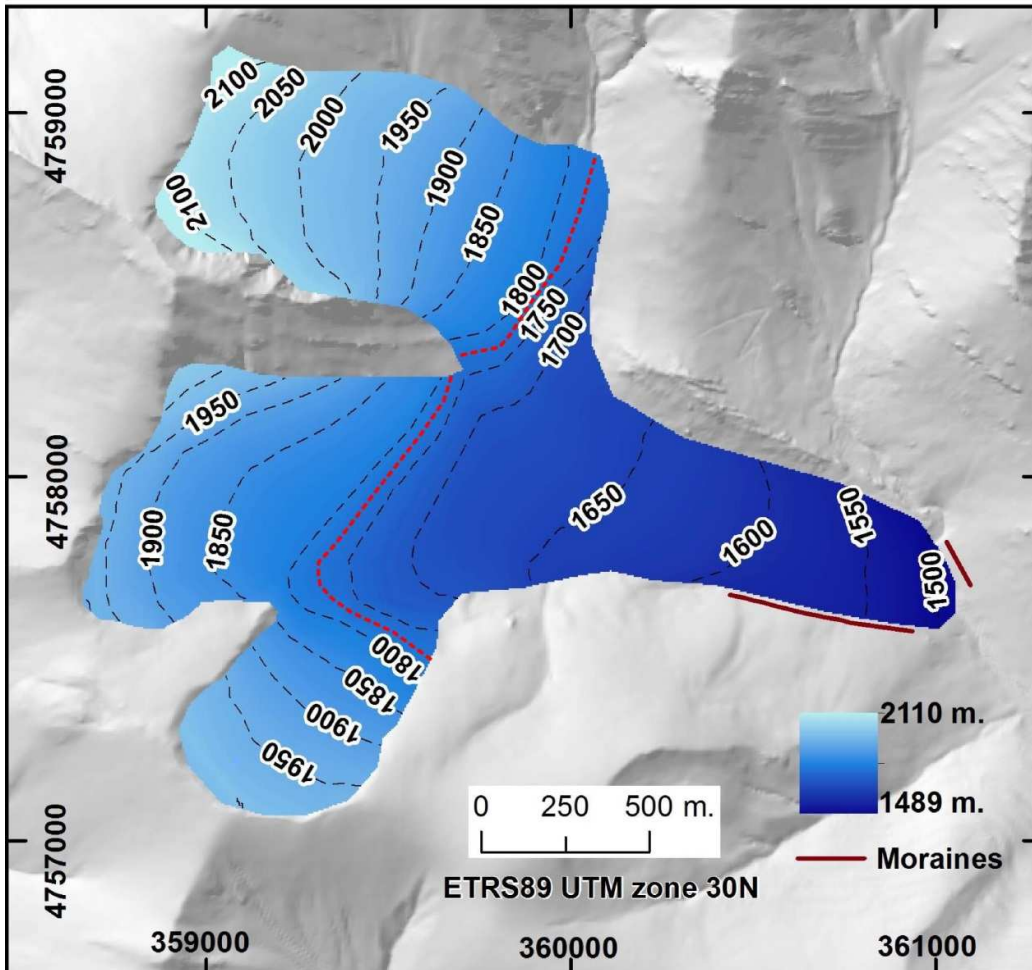
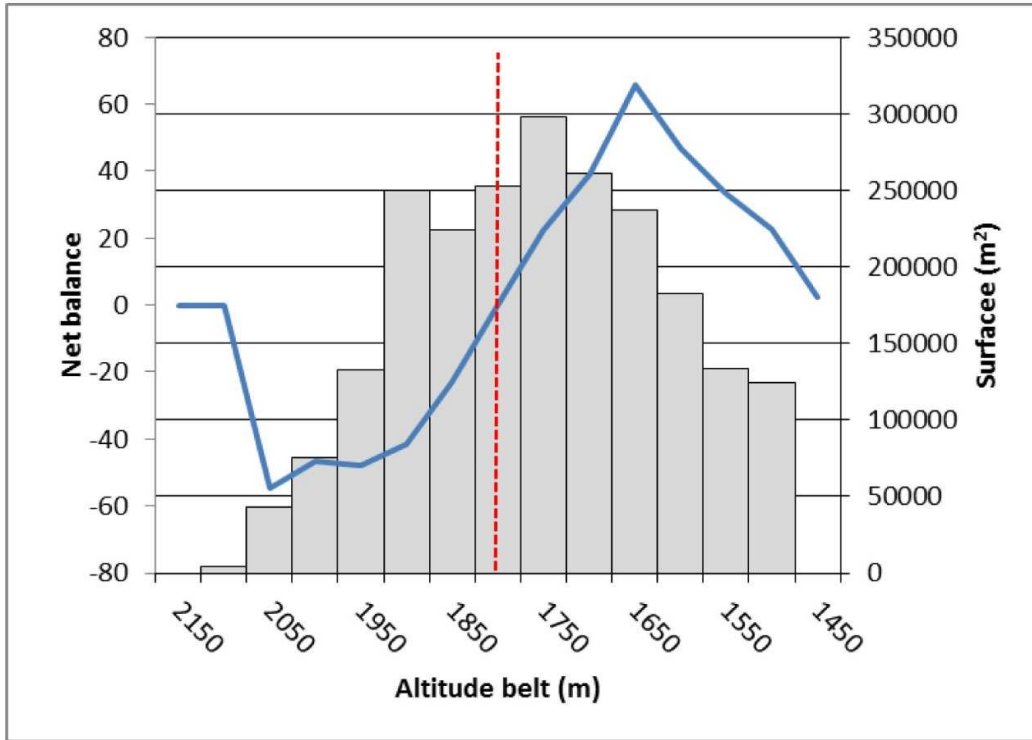
150 A_{ab} = Area of ablation.

151 If there is an extant glacier with a record of measured mass balance, the BR can be determined.
 152 Then, based on assumption (b) above, this is applied to the hypsometry of the reconstructed
 153 palaeoglacier to calculate the palaeo-ELA. This can only be done if the extant glacier is believed to
 154 have similar characteristics to the palaeoglacier (e.g. Rea and Evans, 2007). The next-best alternative
 155 is, provided there are the necessary data, to derive a BR from a nearby glacier and assume the mass
 156 balance is controlled by similar climatic and glaciological boundary conditions. Often neither is
 157 possible because many glacier reconstructions are undertaken in regions that are no longer
 158 glacierized. In these instances, a 'representative' BR has to be chosen, with careful consideration of
 159 additional information, for example, data derived from palaeoecological proxies or perhaps climate
 160 model output, though caution is required here to avoid circularity. Rea (2009) calculated a series of
 161 BRs for a range of glacier types and settings from a global dataset of glaciers which had mass balance
 162 records >7 years. The "representative" BRs are: a global value = 1.75 ± 0.71 ; mid-latitude maritime =
 163 1.9 ± 0.81 ; high-latitude = 2.24 ± 0.85 ; North America – West Coast = 2.09 ± 0.93 ; North America –
 164 Eastern Rockies = 1.11 ± 0.1 ; Canadian Arctic = 2.91 ± 0.35 ; Svalbard = 2.13 ± 0.52 ; Western Norway =

165 1.5± 0.4; European Alps = 1.59±0.6; Central Asia = 1.75±0.56; Kamchatka = 3.18±0.16. Given a
166 population of multiple glaciers within the same region, Osmaston (2005) alternatively suggested
167 performing the calculation for a range of BR's, and then choosing the one with the lowest ELA
168 standard deviation.

169 The AABR calculation is implemented in two steps. First, the glacier surface is divided into contour
170 belts using a reasonable contour interval, and then for each belt the area is multiplied by the mid-
171 point elevation. The sum of these values, derived from all contour belts, is then divided by the total
172 glacier area. This produces the ELA Area-Altitude (AA), which is equivalent to an AABR of 1. For any
173 other BR ratio the second step estimates the ELA by calculating multiple palaeoglacier mass
174 balances, for all possible ELAs, starting at the mid elevation of the lowest contour belt. For each
175 iteration, the trial ELA is subtracted from the mean belt altitude and the result is multiplied by the
176 contour belt area. If the result of the multiplication is negative, then it is multiplied by the BR (i.e. it
177 is in the ablation zone). This is repeated for all contour belts and the results summed to give the
178 glacier net mass balance, which can be either positive or negative. The contour belt where the net
179 balance changes sign, from positive to negative (or vice versa if calculated from the top down), is the
180 ELA for the chosen BR. A new BR value necessitates a new calculation (see Figure 2). For full details
181 of the method see Furbish and Andrews (1984), Benn and Gemmell (1997), Osmaston (2005) and
182 Rea (2009).

ELA AABR 1.75



184 Figure 2. Mass balance calculated using the AABR method using a BR ratio of 1.75 for the same
185 palaeoglacier as in Figure 1. The ELA is located where negative and positive net balances are equal.
186 The vertical bars in the top graphic show the distribution of the glacier area with altitude (the
187 hypsometry), the blue line for its net balance (taking into account the BR) and the red dotted line is
188 the ELA contour, situated at 1775 m (Pellitero, 2012).

189 Various approaches have been used in the past to perform computer-based ELA calculations. Kaser
190 and Osmaston (2002) developed a program to calculate the ELA using the AABR method, which was
191 coded in ALGOL. Later another spreadsheet was made available for the calculation of the AABR
192 (Osmaston 2005). Benn and Gemmell (1997) published an Excel spreadsheet program that also
193 calculated the ELA using the AABR method, but this is unsuitable for glaciers with more extreme
194 hypsometry i.e. large areas towards the top and/or bottom of the accumulation and/or ablation
195 zones respectively (Osmaston, 2005; Rea and Evans, 2007). None of these approaches fully
196 automated the calculation procedure and none used a Geographic Information System (GIS)
197 framework. As a consequence, hypsometry measurements had to be derived separately and
198 imported into a spreadsheet to perform the ELA calculations.

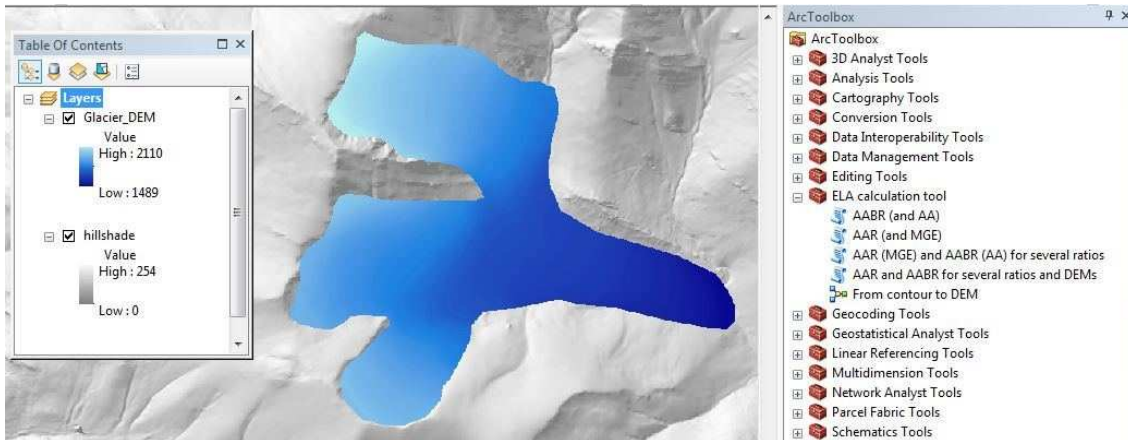
199 **3. The toolbox**

200 This paper presents an ArcGIS toolbox, with Python coded tools, for the automated calculation of
201 the ELA on palaeoglaciers using the four main methods currently in use: the AA (determined as AABR
202 = 1), AAR, AABR and MGE (determined as AAR = 0.5). Computational speed is a function of the
203 contour interval, which is user defined, and the glacier size, though computational times are, at
204 most, in the order of few minutes for a single large valley glacier. The tools follow Osmaston's (2005)
205 procedure for the AABR and González-Trueba and Serrano (2004) approach for the AAR calculation.
206 The toolbox can be downloaded as an attachment to this paper, as well as the source code used, and
207 needs to be added to the general ArcToolbox folder prior to use.

208 **3.1. Toolbox operation, scripts and inputs**

209 The ELA calculation toolbox requires a Digital Elevation Model (DEM) of the glacier surface as the
210 main input and a folder to store the outputs. The DEM can use any of the raster formats supported
211 by ArcGIS 10.1. The toolbox includes four Python coded tools and one model for the creation of the
212 DEM from contour lines (Figure 3). Along with the above the "AAR (and MGE)" and "AABR (and AA)"
213 tools require two additional parameters. The first is the contour interval for the glacier area
214 calculation. The default is set to 50 m, but this can be changed according to user preference. Note it
215 is also dependent on the vertical resolution of the DEM and the size of the glacier; it is pointless
216 selecting a contour interval less than the vertical resolution and a smaller glacier may benefit from a
217 denser spacing of surface contours (e.g. Chandler, 2013). However, a larger contour interval will
218 reduce the vertical accuracy, because the calculation error (i.e. the minimum error) is equal to the
219 chosen contour interval. For example, if the interval is set to 10 m, the resultant ELA calculation
220 error will be ± 5 m. The second key parameter is the ratio for the AAR and AABR methods. Default
221 values of 0.67 for AAR and 1.75 for AABR have been set, following the aforementioned literature,
222 but users are again free to modify this ratio (Figure 4). Once all information is inputted, results are
223 returned in a pop-up window that also contains additional information about the script run (Figure
224 5). A shapefile is created with the contour that corresponds to the ELA. Its name is the same as that
225 of the DEM plus AAR or AABR depending on the tool used.

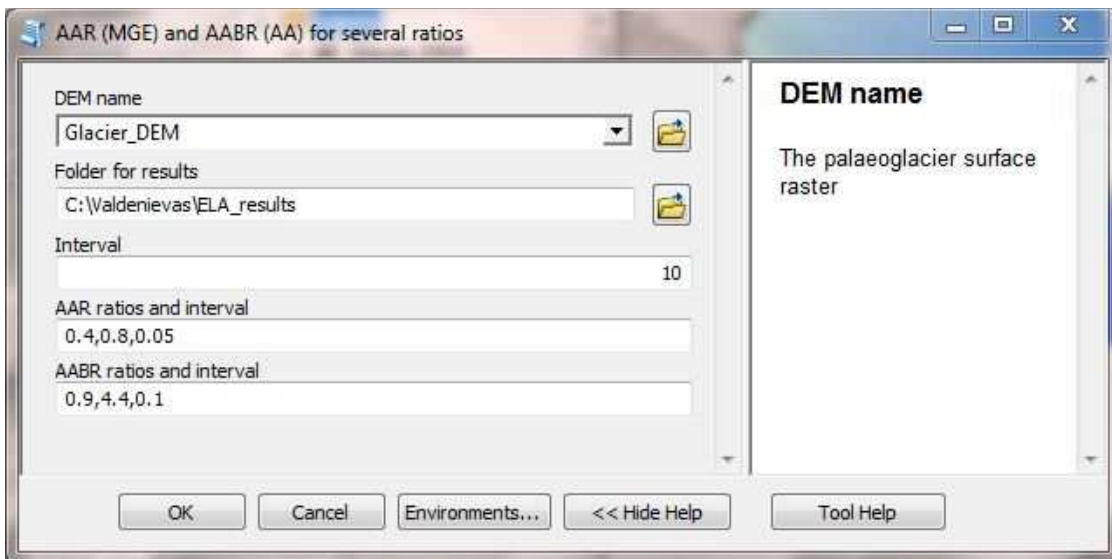
226



227

228 Figure 3. A screenshot of the Toolbox as it appears embedded in ArcGIS.

229 Gonzalez-Trueba and Serrano (2004) suggest introducing a ± 0.05 error in the AAR, which accounts
230 for technical errors in the calculation process. Alternatively, calculating ranges of ELAs is easily
231 implemented using the “AAR and AABR (AA) for several ratios” tool. The tool works in the same way
232 as the previous ones, but two further parameters are added “AAR ratios and interval” and “AABR
233 ratios and interval”. Users can define the range and interval entered thus; *minimum ratio,maximum
234 ratio,interval* (with no spaces between each value). For example, to calculate AAR-ELAs between the
235 ratios 0.4 to 0.7, with 0.05 ratio unit steps, the following is typed “0.4,0.7,0.05”. Default ratio ranges
236 have been set to 0.4-0.8 with a 0.05 interval for AAR, and from 0.9 to 4.4 with a 0.1 interval for
237 AABR, following the proposed ranges for AAR in Kern and Lazlo (2010) and for AABR in Rea (2009)
238 (Figure 4). An AAR of 0.5 (MGE method) is also included as a default. Results are outputted to a *.txt
239 file, saved in the “Workspace” folder, whose name is the same as the DEM plus “_output.txt” and a
240 shapefile taking the DEM name plus “ELAs.shp”.



241

242 Figure 4. An example screenshot of the “AAR and AABR (AA) for several ratios” tool as it appears
243 when opened from the toolbox.

244 The tool “AAR and AABR (AA) multiple ratios and DEMs” allows ELA calculations for multiple DEMs
245 stored in the same folder, using multiple ratios for both the AAR and AABR methods. The only
246 required inputs are the relevant folder (named as “Workspace” in the tool) where the DEMs are
247 stored (and where results will be eventually output too), the contour interval for the glacier contour
248 belt areas and the ratio ranges for AAR and AABR. Results are saved in a text file called
249 “ELA_values_AAR_and_AABR.txt”. Finally, the best ELA for the group of glaciers, determined using
250 the lowest standard deviation approach proposed by (Osmaston 2005), is provided at the end of the
251 results text file (Figure 5). Note that if the tool is re-run in the same folder, results are appended at
252 the end of the text file already created. An ELA shapefile is also created for each DEM, which is
253 named following the same convention as above.

```
File Edit Format View Help
values for raster gorjnice
The ELA AAR at ratio 0.6 is: 1454
The ELA AAR at ratio 0.7 is: 1444
The ELA AAR at ratio 0.8 is: 1434
The ELA MGE is: 1474
The ELA AA is: 1486.667552159912
The ELA AABR at ratio 0.9 is: 1489.0
The ELA AABR at ratio 1.0 is: 1489.0
The ELA AABR at ratio 1.1 is: 1489.0
values for raster lijevnoice
The ELA AAR at ratio 0.6 is: 1915
The ELA AAR at ratio 0.7 is: 1915
The ELA AAR at ratio 0.8 is: 1905
The ELA MGE is: 1925
The ELA AA is: 1915.4445985513946
The ELA AABR at ratio 0.9 is: 1920.0
The ELA AABR at ratio 1.0 is: 1920.0
The ELA AABR at ratio 1.1 is: 1910.0
values for raster saraseice
The ELA AAR at ratio 0.6 is: 2379
The ELA AAR at ratio 0.7 is: 2369
The ELA AAR at ratio 0.8 is: 2369
The ELA MGE is: 2379
The ELA AA is: 2375.689790255448
The ELA AABR at ratio 0.9 is: 2374.0
The ELA AABR at ratio 1.0 is: 2374.0
The ELA AABR at ratio 1.1 is: 2374.0
The minimum standard deviation ELA for AAR method is
331 meters at a ratio of 0.8 and an average of 1999.0 meters
The minimum standard deviation ELA for AABR method is
333 meters at a ratio of 1.0 and an average of 2044.0 meters
For Osmaston (2006) ELA retrieval, user is advised to assume that
all glaciers included are coetaneous
```

254

255 Figure 5. Example output for “AAR and AABR (AA) several ratios and DEMs” script.

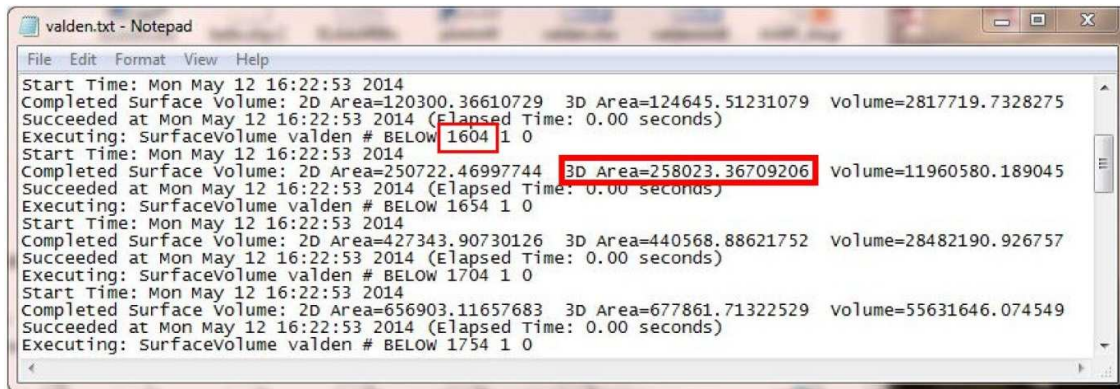
256 In addition, there is a model for the creation of a DEM from contours, which may be useful for users
257 who are unfamiliar with spatial analysis in ArcGIS. This is not coded in Python, but built through the
258 Model Builder directly in ArcGIS. The model uses the “Topo to Raster” tool and requires three inputs:
259 the glacier contours shapefile, the glacier outline and the name and location for the resulting DEM.
260 The first input must be a POLYLINE shapefile or feature class with a field named “CONTOUR”,
261 populated with the elevation of each contour (in m above sea level). The second input is the glacier
262 outline, which can be either, a POLYLINE or, a POLYGON. The third input is the name and location for
263 the output DEM.

264

265 3.2. Script execution

266 All scripts are coded in Python 2.7 and use *arcpy* (ESRI toolset for Python), *os*, *numpy* and *operator*
267 libraries. They mainly utilise the SurfaceVolume_3D tool, which is embedded in the 3D Analyst

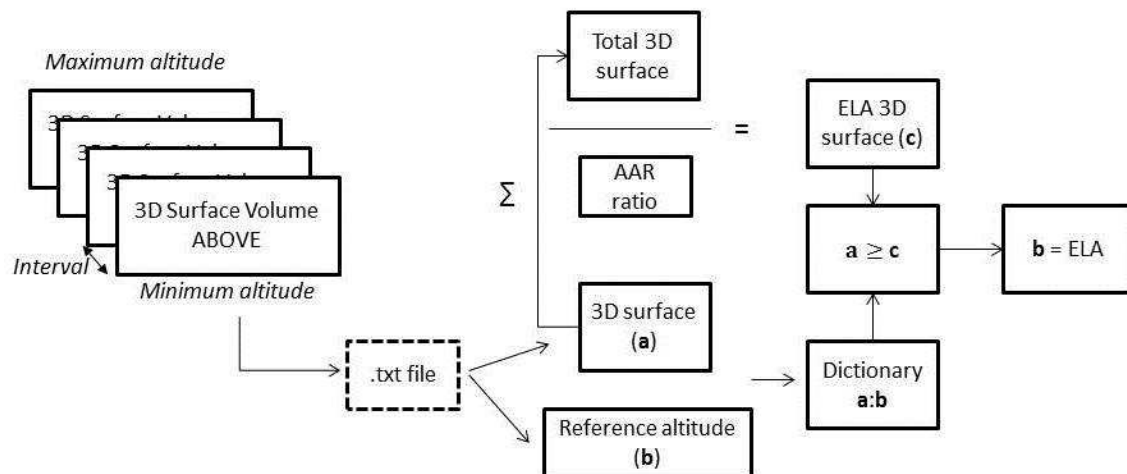
268 package. This tool calculates the 3D area ABOVE or BELOW a given altitude in a DEM. The script first
 269 runs the tool to calculate the area ABOVE (for AAR) and BELOW (for AA and AABR) the “trial”
 270 altitudes as many times as needed given the glacier altitudinal range (which is automatically
 271 calculated) and the desired contour interval. Results are recorded in a .txt file which is named from
 272 the DEM and stored in the chosen folder. Then, the script reads the relevant information from the
 273 text file and calculates the ELA. Two values are used for the calculation: the reference altitude and
 274 the area value for that altitude (Figure 6).



275

276 Figure 6. Results from the SurfaceVolume_3D tool. Reference altitude (1604 m.) and 3D area below
 277 this altitude (258,023 m²) values have been outlined. These are the values that the script uses for
 278 performing the ELA calculations.

279 For the AAR both values are stored in a dictionary, and then the accumulation area (the area above
 280 the ELA which is relevant for the given ratio) is calculated from the total area and the chosen ratio.
 281 Finally the script goes through the dictionary and finds the contour above which the cumulative
 282 area value is immediately higher than the accumulation area, and determines the mean value between
 283 this contour altitude and the one below. This yields an altitude value whose ELA calculation error is
 284 half the contour interval used (Figure 7).

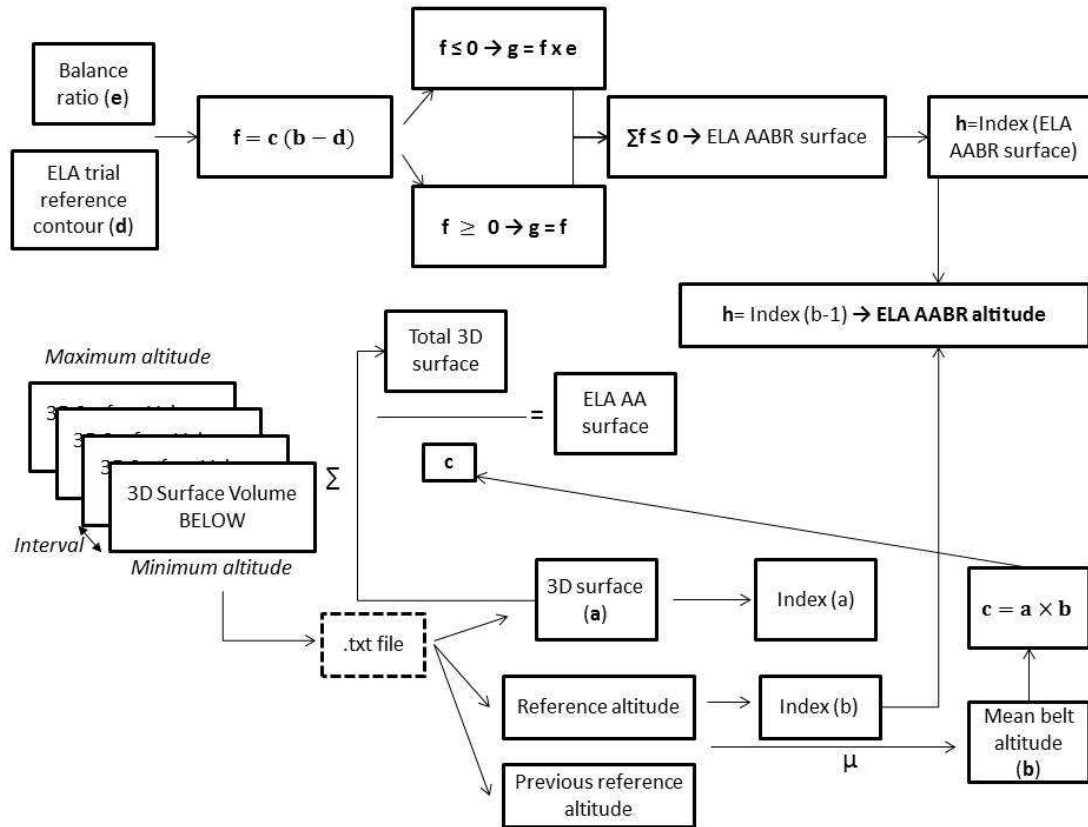


285

286 Figure 7. Flow-diagram illustrating the steps in ELA calculation using the AAR method.

287 For the AABR the glacier is split into contour belts, so the distribution of surface area with elevation
 288 above and below the ELA is taken into account (the strength of this method). First the script
 289 calculates the total area BELOW each contour, and then creates a list of the mean altitude value for
 290 each contour belt. The surface area for each belt is calculated by iteratively subtracting the area
 291 below the upper contour from the area below the contour directly below, and the result is
 292 multiplied by the mean altitude of the belt. All results are summed and then divided by the total
 293 area of the glacier. The result is the AA value, which is equivalent to the AABR for a BR of 1.

294 In order to calculate ELAs using BRs other than unity, the script performs some further calculations,
 295 following Osmaston (2005): a trial ELA is created and is then subtracted from the mean contour belt
 296 altitude for all belts (i.e. the elevation of each contour belt from the trial ELA is determined –
 297 negative for contour belts below the trial ELA and positive above) and multiplied by each contour
 298 belt area. Negative values are multiplied by the chosen BR (i.e. they are in the ablation zone). All belt
 299 area-altitude-BR products are added, yielding a result which is initially positive, but decreases on
 300 iterating upwards. The first time the result becomes negative means that the zero net balance ELA
 301 is situated in the belt below the trial ELA (Figure 9). The script outputs the ELA as the mean altitude of
 302 this belt, so again the calculation error is, at most, equal to half the contour interval.



303

304 Figure 8. Schematic flow-diagram showing the steps taken in ELA calculation procedure for the
 305 AA/AABR method.

306 The scripts are commented, so users can follow their rationale and, should they wish, adapt them to
 307 their needs.

308 **3.3. Software requirements**

309 This toolbox is intended to work within ArcGIS 10.1 and subsequent versions. A 3D Analyst and
310 Spatial Analyst license is also required.

311

312 **4. Some tips for glacier reconstruction**

313 The “accuracy” of the ELA calculation can be quantified but the overall “quality” is highly dependent
314 on the palaeoglacier surface reconstruction. There are two main methods used to generate a glacier
315 surface using landform evidence. The first is achieved by reconstructing the ice thickness along a
316 flowline using an equation for ice rheology, following Nye (1952), which was adapted by Schilling
317 and Hollin (1981) and Benn and Hulton (2010), with the latter authors producing a useful Excel
318 spreadsheet. An automated approach for this, implemented in ArcGIS, is currently in preparation
319 (Frew et al., in prep.). The alternative is the cartographic approach, which relies on the “skill and
320 knowledge” of the scientist to interpret a glacier surface using geomorphological evidence by
321 drawing contours which replicate “typical ice surfaces” observed today. The latter option becomes
322 problematic where landform evidence disappears and where no topographical constraint limits the
323 ice thickness e.g. for icecaps and icefields (Rea et al. 1999). In such cases the physical based
324 modelling provides the only constraint on the palaeoglacier geometry.

325 **5. Conclusions**

326 This tool provides a method for the calculation of zero net balance/equilibrium ELAs using the four
327 most used methods in palaeoglaciology and provides rapid calculations for single or multiple glacier
328 datasets. It is intended to be useable by both those familiar with ArcGIS and novices alike. The Tool
329 and source code can be downloaded with the paper and so can be modified to meet other end-user
330 needs. The tool and source code is also available from the lead authors.

331 **Acknowledgements**

332 This research has been supported by the Leverhulme Trust International Network Grant IN-2012-
333 140. We acknowledge the very helpful comments of Doug Benn and an anonymous reviewer on an
334 earlier draft of this paper.

335 **Bibliography**

336 Ahlmann, H.W., 1924. The glaciation level as a function of humidity accumulation in a solid form.
337 *Geografiska Annaler* 6, 223–272 [in French].

338 Ahlmann, H.W., 1948. *Glaciological Research on the North Atlantic Coasts*. Royal Geographical
339 Society, London, 83 pp.

340 Bakke, J., Dahl, S.O., Nesje, A., 2005. Lateglacial and early Holocene palaeoclimatic reconstruction
341 based on glacier fluctuations and equilibrium-line altitudes at northern Folgefonna, Hardanger,
342 western Norway. *Journal of Quaternary Science* 20, 179–198.

343 Bakke, J., Nesje, A., 2011. Equilibrium-Line Altitude (ELA). Encyclopedia of Snow, Ice and Glaciers.
344 Singh, V.; Singh, P. & Haritashya, U. (Eds.). Springer, Netherlands, 268-277

345 Ballantyne, C.K., 1989. The Loch Lomond Readvance on the Isle of Skye, Scotland: glacier
346 reconstruction and palaeoclimatic implications. *Journal of Quaternary Science* 4, 95-108.

347 Barr, I., Spagnolo, M., 2014. Testing the efficacy of the glacial buzzsaw: insights from the Sredinny
348 Mountains, Kamchatka. *Geomorphology*, 206: 230–238.

349 Benn, D. I., Gemmel, A. M. D., 1997. Calculating equilibrium-line altitudes of former glaciers by the
350 balance ratio method: a new computer spreadsheet. *Glacial Geology and Geomorphology*, 7
351 (<http://ggg.qub.ac.uk/papers/full/1997/tn011997/tn01.html>).

352 Benn, D.I., Lehmkuhl, F., 2000. Mass balance and equilibrium line altitudes of glaciers in high
353 mountain environments. *Quaternary International* 65/66, 15–29.

354 Benn, D. I. and Ballantyne, C. K., 2005. Palaeoclimatic reconstruction from Loch Lomond Readvance
355 glaciers in the West Drumochter Hills, Scotland. *Journal of Quaternary Sciences*, 20, 577–592.

356 Benn, D.I., Hulton, N.R.J., 2010. An Excel™ spreadsheet program for reconstructing the surface
357 profile of former mountain glaciers and ice caps. *Computers & Geosciences*, 36, 605-610.

358 Braithwaite, R.J., Müller, F. 1980. On the parameterization of glacier equilibrium line altitude. IAHS
359 Publ. 126 (Riederalp Workshop 1978 – World Glacier Inventory), pp. 263–271.

360 Braithwaite, R. J., 1985. Calculation of degree-days for glacier-climate research. *Zeitschrift für*
361 *Gletscherkunde und Glazialgeologie* 20, 1-8.

362 Braithwaite, R.J. and Raper, S.C.B., 2007. Glaciological conditions in seven contrasting regions
363 estimated with the degree-day model. *Annals of Glaciology*, 46 (1): 297-302.

364 Braithwaite, R. J., 2008. Temperature and precipitation climate at the equilibrium-line altitude of
365 glaciers expressed by the degree-day factor for melting snow. *Journal of Glaciology* 54 (186), 437-
366 444.

367 Braithwaite, R.J., Raper, S.C.B., 2009. Estimating equilibrium-line altitude (ELA) from glacier inventory
368 data. *Annals of Glaciology*, 50 (53), 127-132.

369 Carr, S.J., Coleman, C.G. 2007. An improved technique for the reconstruction of former glacier mass-
370 balance and dynamics. *Geomorphology* 92(1–2): 76–90.

371 Carr, S.J., Lükar, S., Mills, S.C., 2010. Glacier reconstruction and mass-balance modelling as a
372 geomorphic and palaeoclimatic tool. *Earth Surface Processes and Landforms*, 35, 1103–1115.

373 Chandler, B.M.P., 2013. Glacial geomorphology of Ben More Coigach, Northwest Scottish Highlands:
374 Implications for Loch Lomond Stadial glaciation and palaeoclimate. Unpublished BSc dissertation,
375 Queen Mary University of London, 110 pp.

376 Clark, D.H., Clark, M.M., Gillespie, A.R., 1994. Debris-covered glaciers in the Sierra Nevada,
377 California, and their implications for snowline reconstructions. *Quaternary Research*, 41, 139-153.

378 Cogley, J.G., R. Hock, L.A. Rasmussen, A.A. Arendt, A. Bauder, R.J. Braithwaite, P. Jansson, G. Kaser,
379 M. Möller, L. Nicholson and M. Zemp, 2011, Glossary of Glacier Mass Balance and Related Terms,
380 IHP-VII Technical Documents in Hydrology No. 86, IACS Contribution No. 2, UNESCO-IHP, Paris.

381 Drygalski, E., 1942. *Glaciology*. Franz Deutich, Vienna. 258pp.[in German]

382 Egholm, D.L., Nielsen, S.B., Pedersen, V.K., Lesemann, J.E., 2009. Glacial effects limiting mountain
383 height. *Nature* 460, 884–887

384 Furbish, D.J., Andrews, J.T., 1984. The use of hypsometry to indicate long term stability and response
385 of valley glaciers to changes in mass transfer. *Journal of Glaciology*, 30, 199–211.

386 González Trueba, J.J. and Serrano, E., 2004. The AAR method for palaeo-ELA determination:
387 methodological analysis and application to Valdecebollas Massif (Cantabrian Range). *Cuadernos de*
388 *Investigación Geográfica*, 30, 7-34 [in Spanish].

389 Gray, J.M., 1982. The last glaciers (Loch Lomond Advance) in Snowdonia, North Wales. *Geological*
390 *Journal*, 17, 111-133.

391 Gross, G., Kerschner, H., Patzelt, G., 1978. Methodological studies of the snow line in alpine glaciers.
392 *Zeitschrift für Gletscherkunde und Glazialgeologie*, 12, 223-251 [in German].

393 Hagen, J.O., Lefauconnier, B., Liestøl, O., 1991. Glacier mass balance in Svalbard since 1912. In:
394 Kotlyakov, V.M., Ushakov, A., Glazovsky, A. (Eds.), *Glaciers–Ocean– Atmospheric Interactions*, vol.
395 208. IAHS Publication, Great Yarmouth, United Kingdom, pp. 313–328.

396 Hughes, P.D., 2002. Loch Lomond Stadial glaciers in the Aran and Arenig Mountains, North Wales,
397 Great Britain. *Geological Journal*, 37, 9-15.

398 Hughes, P.D., 2009a. Twenty-first Century Glaciers and Climate in the Prokletije Mountains, Albania.
399 *Arctic, Antarctic and Alpine Research*, 41 (4), 455-459.

400 Hughes, P.D., 2009b. Loch Lomond Stadial (Younger Dryas) glaciers and climate in Wales. *Geological*
401 *Journal*, 44, 375-391.

402 Hughes, P.D., Woodward, J.C., Gibbard, P.L., 2007. Middle Pleistocene cold stage climates in the
403 Mediterranean: new evidence from the glacial record. *Earth and Planetary Science Letters*, 253, 50-
404 56.

405 Hughes, P.D., Woodward, J.C., van Calsteren, P.C., Thomas, L.E., Adamson, K.R., 2010. Pleistocene ice
406 caps on the coastal mountains of the Adriatic Sea. *Quaternary Science Reviews*, 19, 3690-3708.

407 Ignéczi, A. and Nagy, B., 2013. Determining steady-state accumulation-area ratios of outlet glaciers
408 for application of outlets in climate reconstructions. *Quaternary International*, 293, 268-274.

409 Kaser, G. and Osmaston, H.A., 2002. *Tropical glaciers*. Cambridge University Press, Cambridge.

410 Kerschner, H., Kaser, G., Sailer, R., 2000. Alpine Younger Dryas glaciers as palaeo-precipitation
411 gauges. *Annals of Glaciology*, 31, 80-84.

412 Kern, Z. and László, P., 2010. Size specific steady-state accumulation-area ratio: an improvement for
413 equilibrium-line estimation of small palaeoglaciers. *Quaternary Science Reviews*, 29: 2781 – 2787.

414 Krenke, A.N. and Khodakov, V.G., 1966. The relationship between surface ice melting and air
415 temperature. *Materialy Glyatsiologicheskikh Issledovanií* 12, 153–164. [In Russian]

416 Kurowski, L., 1891. The amount of snow limit with special emphasis on the Finsterahorn group.
417 *Geographische Abhandlungen*, 5 (1), 115-160 [in German].

418 Lichtenecker, N., 1938. The current and the glacial snow line in the eastern Alps. In: *Verhandl.d.III.*
419 *Intern. Quartär-Konferenz, Wien*, 141-147 [in German].

420 Leonard, E.M., 1984. Late Pleistocene equilibrium-line altitudes and modern snow accumulation
421 patterns, San Juan Mountains, Colorado, U.S.A. *Arctic and Alpine Research*, 16, 65-76.

422 Lichtenecker, N., 1938. Die gegenwärtige und die eiszeitliche Schneegrenze in den Ostalpen.
423 *Verhandlungen der III Internationalen Quartarkonferenz*, Wien, 141-47.

424 Loewe, F., 1971. Considerations of the origin of the Quaternary ice-sheet in North America. *Arctic*
425 *and Alpine Research*, 3, 331–344.

426 Lukas, S., 2007. Early-Holocene glacier fluctuations in Krundalen, south central Norway: palaeo-
427 glacier dynamics and palaeoclimate. *The Holocene*, 17, 585-598.

428 Lukas, S.,Bradwell, T., 2010. Reconstruction of a Lateglacial (Younger Dryas) mountain icefield in
429 Sutherland, northwestern Scotland, and its palaeoclimatic implications. *Journal of Quaternary*
430 *Science*, 25, 567–580.

431 Meierding, T. C., 1982. Late Pleistocene glacial equilibrium-line in the Colorado Front Range: a
432 comparison of methods. *Quaternary Research*, 18, 289–310.

433 Müller, F., 1980. Present and late Pleistocene equilibrium line altitudes in the Mt Everest region - an
434 application of the glacier inventory. *International Association of Hydrological Sciences Publication*,
435 126, 75-94.

436 Müller, F., Caflisch T.,G. Müller., 1977. Instructions for the compilation and assemblage of data for a
437 world glacier inventory. Zürich, ETH Zürich. Temporary Technical Secretariat for the World Glacier
438 Inventory, 22 pp.

439 Nye, J.F., 1952. The mechanics of glacier flow. *Journal of Glaciology*, 2, 82–93.

440 Porter, S.C., 2001. Snowline depression in the tropics during the Last Glaciation. *Quaternary Science*
441 *Reviews*, 20, 1067-1091.

442 Ohmura, A., Kasser, P., Funk, M., 1992. Climate at the equilibrium line of glaciers. *Journal of*
443 *Glaciology*, 38 (130), 397-411.

444 Osmaston, H., 1965. The Past and Present Climate and Vegetation of Ruwenzori and its
445 neighbourhood. D.Phil thesis, University of Oxford. 238 pp.

- 446 Osmaston, H., 1975. Models for the estimation of firnlines of present and Pleistocene Glaciers. In:
447 Peel, R.F., Chisholm, M.D.I., Haggett, P. (Eds.), *Processes in Physical and Human Geography*, Bristol
448 *Essays* (1975), pp. 218–245.
- 449 Osmaston, H., 2002. Chapter 9. The nature, extents and climates of former Quaternary tropical
450 glaciers, with reference to the East African Mountains. In Kaser, G. and Osmaston, H. (eds) *Tropical*
451 *Glaciers*. Cambridge University Press: Cambridge. p. 149-192.
- 452 Osmaston, H., 2005. Estimates of glacier equilibrium line altitudes by the area x altitude, the area x
453 altitude balance ratio and the area x altitude balance index methods and their validation.
454 *Quaternary International*, 138, 22–31.
- 455 Pellitero, R., 2012. *Geomorphology, Quaternary palaeoenvironment and geodiversity of Fuentes*
456 *Carrionas Massif-Montaña Palentina*. PhD Thesis. University of Valladolid, 1085 pp [in Spanish].
- 457 Pellitero, R., 2013. Lateglacial evolution of Fuentes Carrionas massif (Cantabrian
458 Range), palaeoenvironmental and chronological estimations. *Cuaternario y Geomorfología*, 27 (1-2),
459 71-90 [in Spanish].
- 460 Pewé, T.L., Reger, R.D., 1972. Modern and wisconsinan snowlines in Alaska. In: *Proceeding of the*
461 *XXIV International Geological Congress*, secc. 12, 187-197.
- 462 Porter, S., 2001. Snowline depression in the tropics during the Last Glaciation. *Quaternary Science*
463 *Reviews*, 20, 1067-1091.
- 464 Rea, B. R., 2009. Defining modern day area-altitude balance ratios (AABRs) and their use in glacier-
465 climate reconstructions. *Quaternary Science Reviews*, 28(3–4), 237–248.
- 466 Rea, B.R., Evans, D.J.A.. 2007. Quantifying climate and glacier mass balance in north Norway during
467 the Younger Dryas. *Palaeogeography, Palaeoclimatology, Palaeoecology*, 246, 307-330.
- 468 Rea, B.R., Whalley, W.B., Dixon, T., Gordon, J.E., 1999. Plateau icefields as contributing areas to valley
469 glaciers and the potential impact on reconstructed ELAs: a case study from the Lyngen Alps, North
470 Norway. *Annals of Glaciology*, 28, 97-102.
- 471 Schilling, D.H., Hollin, J.T., 1981. Numerical reconstructions of valley glaciers and small ice caps. In:
472 Denton, G.H., Hughes, T.J. (Eds.), *The Last Great Ice Sheets*. Wiley, New York, pp. 207-220.
- 473 Sissons, J.B., 1974. Palaeoclimatic inferences from former glaciers in Scotland and the Lake District.
474 *Nature*, 278, 518 521.
- 475 Stansell, N.D., Polissar, P.J., Abbott, M.B., (2007). Last glacial maximum equilibrium-line altitude and
476 paleo-temperature reconstructions for the Cordillera de Mérida, Venezuelan Andes. *Quaternary*
477 *Research*, 67, 115-127.
- 478 Sutherland, D.G., 1984. Modern glacier characteristics as a basis for inferring former climates with
479 particular reference to the Loch Lomond Stadial. *Quaternary Science Reviews*, 3, 291-309.

Figure 1

[Click here to download high resolution image](#)

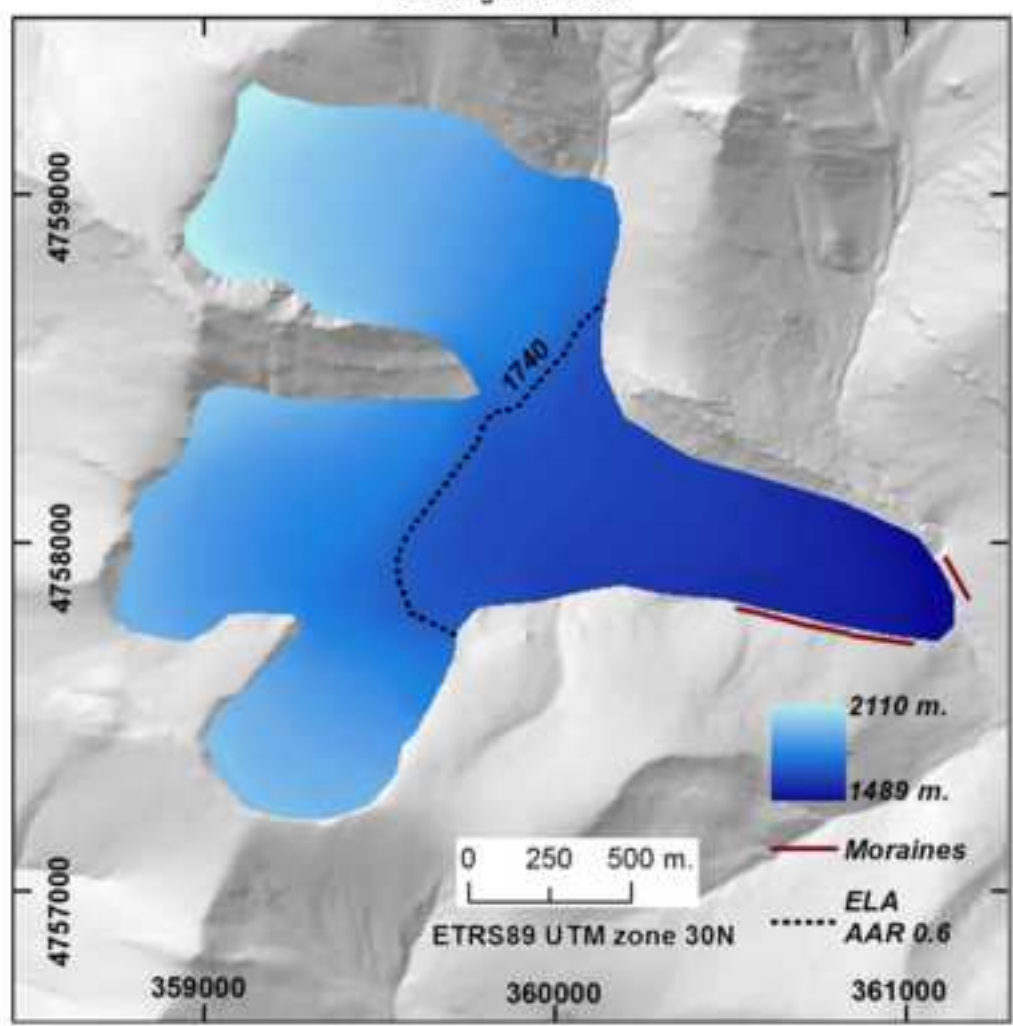
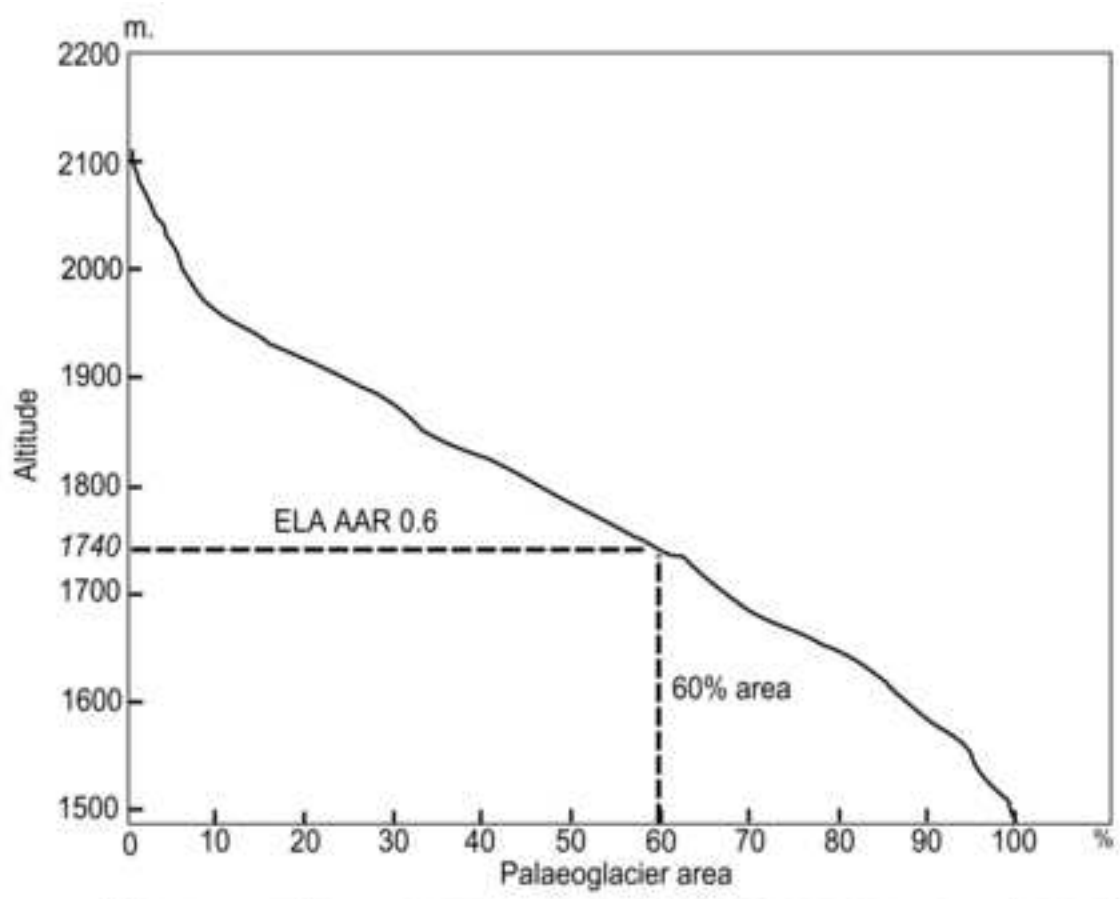


Figure 2

[Click here to download high resolution image](#)

ELA ABR 1.78

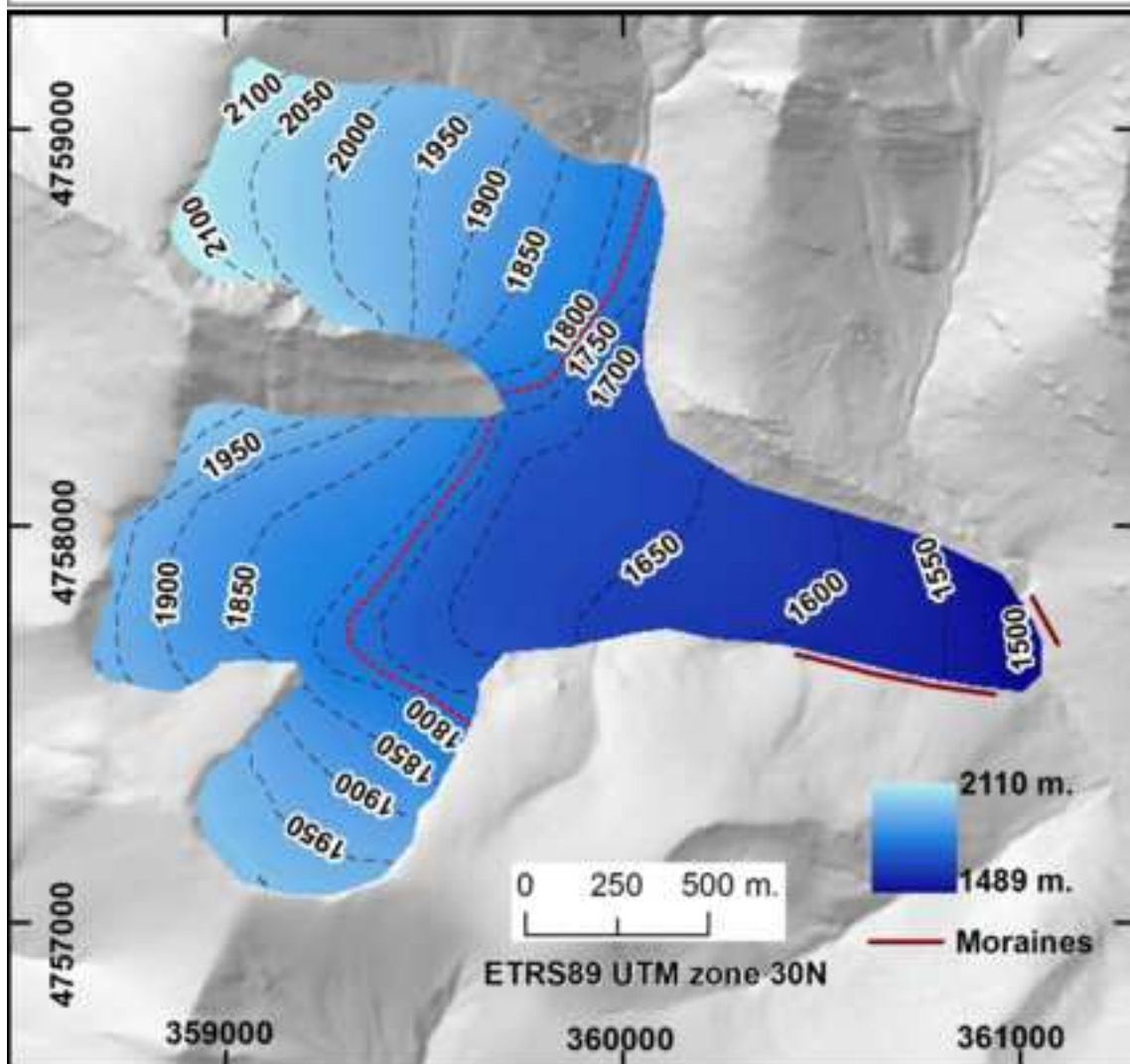
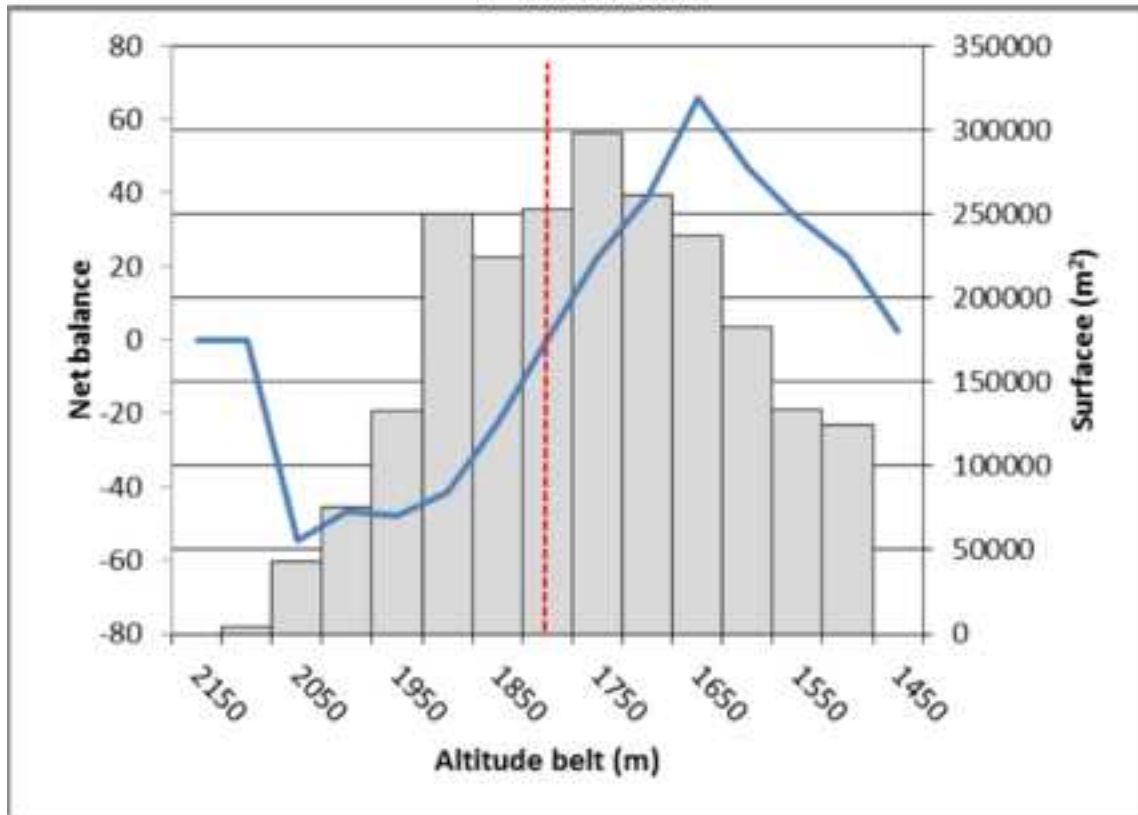


Figure 3
[Click here to download high resolution image](#)

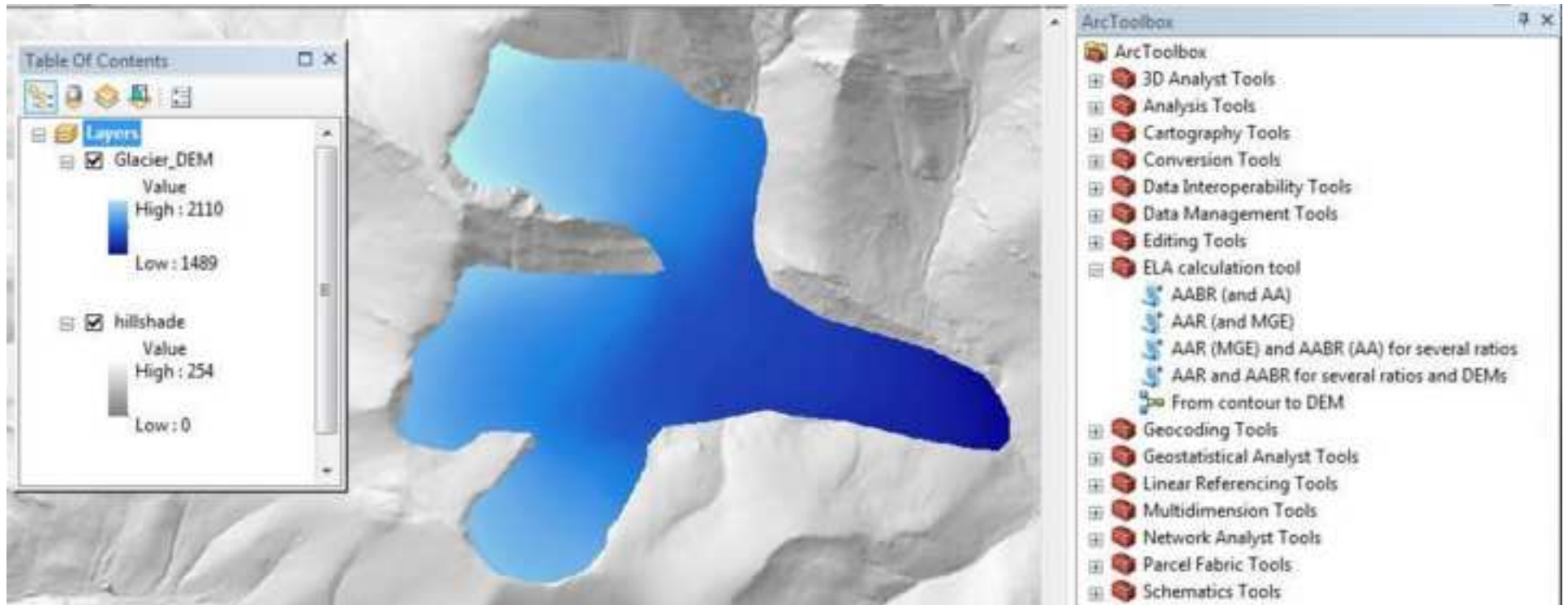


Figure 4
[Click here to download high resolution image](#)

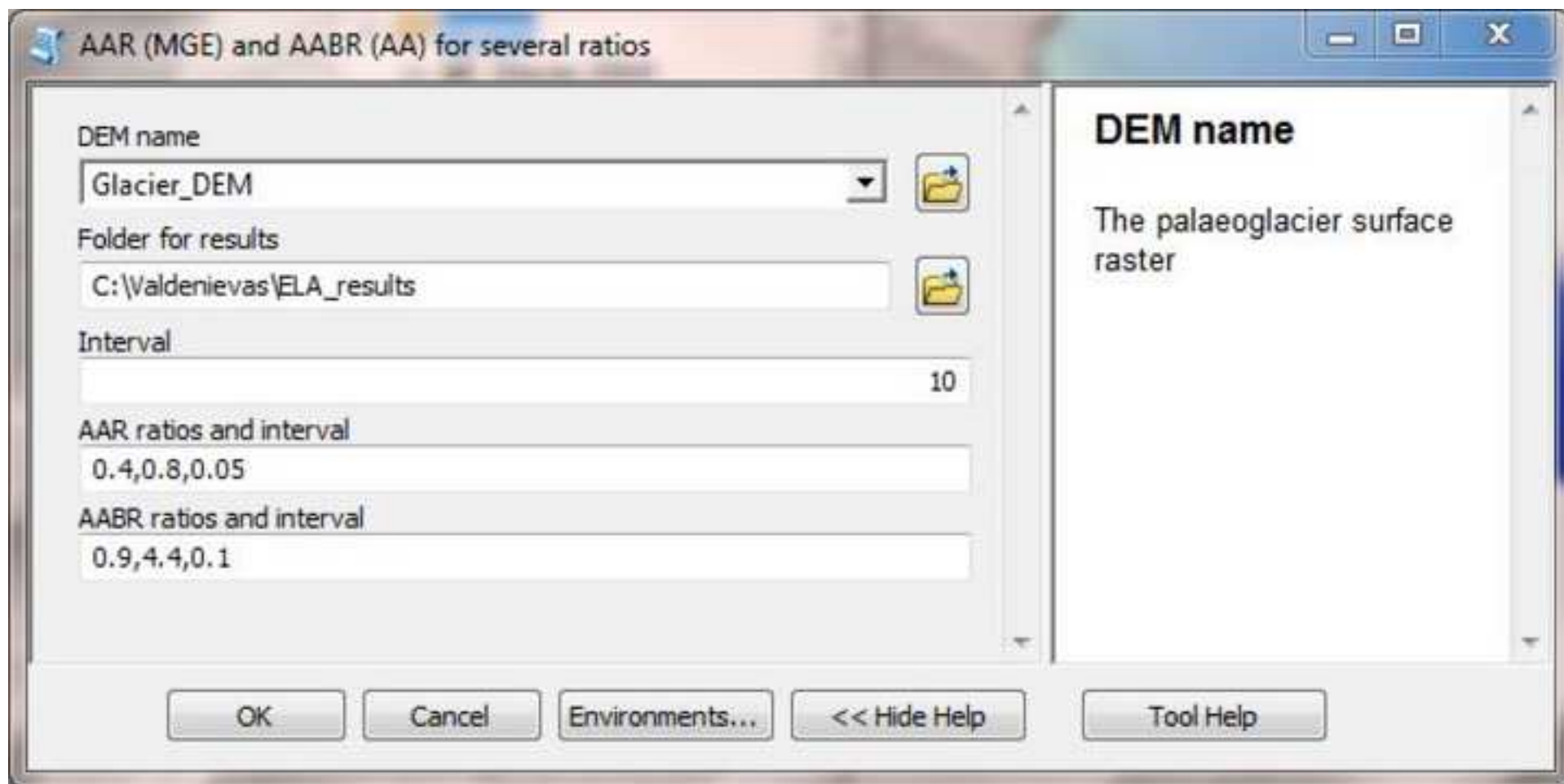
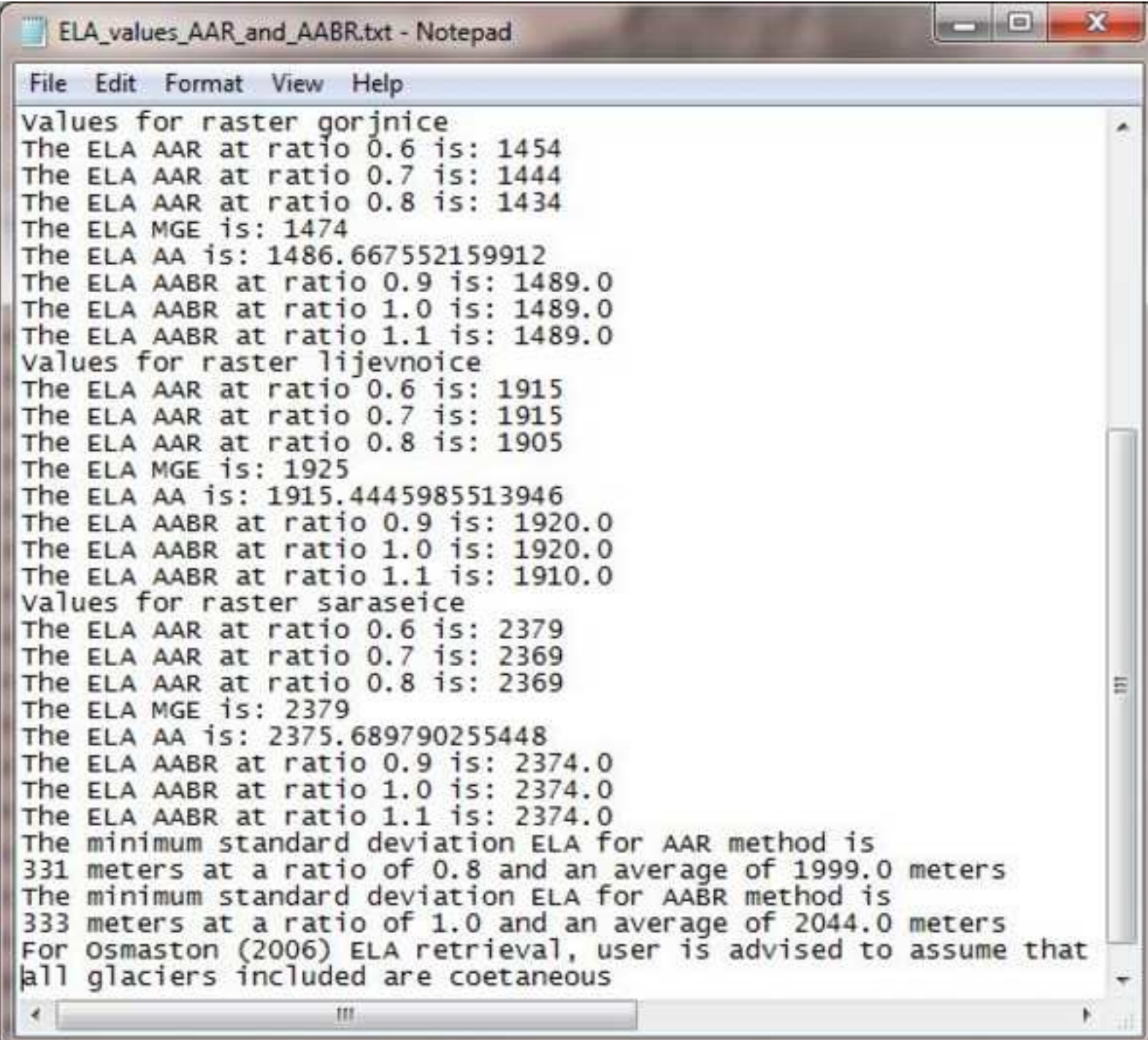


Figure 5

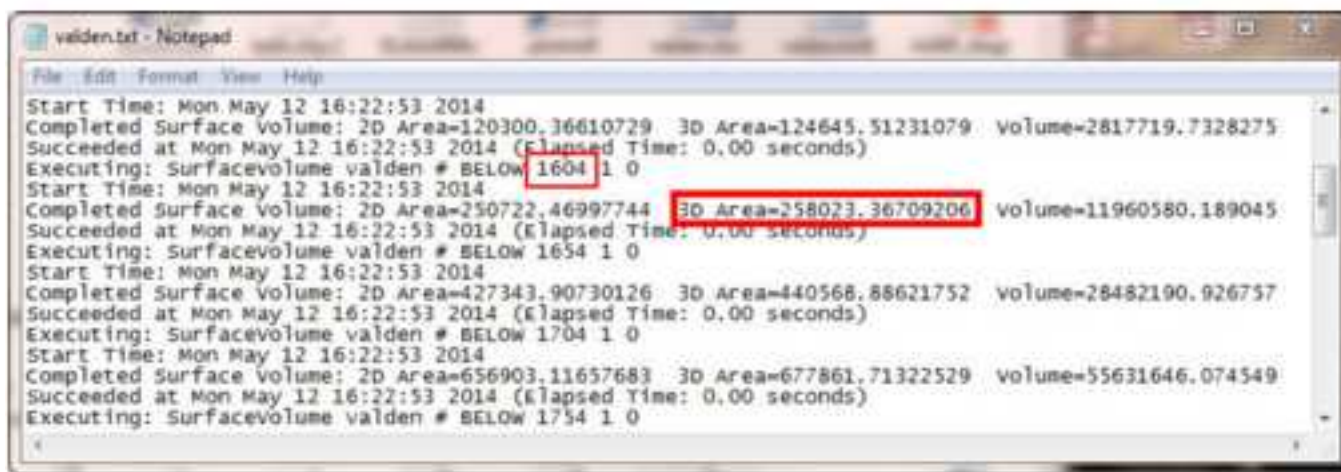
[Click here to download high resolution image](#)



```
ELA_values_AAR_and_AABR.txt - Notepad
File Edit Format View Help
Values for raster gorjnice
The ELA AAR at ratio 0.6 is: 1454
The ELA AAR at ratio 0.7 is: 1444
The ELA AAR at ratio 0.8 is: 1434
The ELA MGE is: 1474
The ELA AA is: 1486.667552159912
The ELA AABR at ratio 0.9 is: 1489.0
The ELA AABR at ratio 1.0 is: 1489.0
The ELA AABR at ratio 1.1 is: 1489.0
Values for raster lijevnoice
The ELA AAR at ratio 0.6 is: 1915
The ELA AAR at ratio 0.7 is: 1915
The ELA AAR at ratio 0.8 is: 1905
The ELA MGE is: 1925
The ELA AA is: 1915.4445985513946
The ELA AABR at ratio 0.9 is: 1920.0
The ELA AABR at ratio 1.0 is: 1920.0
The ELA AABR at ratio 1.1 is: 1910.0
Values for raster saraseice
The ELA AAR at ratio 0.6 is: 2379
The ELA AAR at ratio 0.7 is: 2369
The ELA AAR at ratio 0.8 is: 2369
The ELA MGE is: 2379
The ELA AA is: 2375.689790255448
The ELA AABR at ratio 0.9 is: 2374.0
The ELA AABR at ratio 1.0 is: 2374.0
The ELA AABR at ratio 1.1 is: 2374.0
The minimum standard deviation ELA for AAR method is
331 meters at a ratio of 0.8 and an average of 1999.0 meters
The minimum standard deviation ELA for AABR method is
333 meters at a ratio of 1.0 and an average of 2044.0 meters
For Osmaston (2006) ELA retrieval, user is advised to assume that
all glaciers included are coetaneous
```

Figure 6

[Click here to download high resolution image](#)



```
valden.txt - Notepad
File Edit Format View Help
Start Time: Mon May 12 16:22:53 2014
Completed Surface Volume: 2D Area=120300.36610729 3D Area=124645.51231079 volume=2817719.7328275
Succeeded at Mon May 12 16:22:53 2014 (Elapsed Time: 0.00 seconds)
Executing: Surfacevolume valden # BELOW 1604 1 0
Start Time: Mon May 12 16:22:53 2014
Completed Surface Volume: 2D Area=250722.46997744 3D Area=258023.36709206 volume=11960580.189045
Succeeded at Mon May 12 16:22:53 2014 (Elapsed Time: 0.00 seconds)
Executing: Surfacevolume valden # BELOW 1654 1 0
Start Time: Mon May 12 16:22:53 2014
Completed Surface Volume: 2D Area=427343.90730126 3D Area=440568.88621752 volume=28482190.926757
Succeeded at Mon May 12 16:22:53 2014 (Elapsed Time: 0.00 seconds)
Executing: Surfacevolume valden # BELOW 1704 1 0
Start Time: Mon May 12 16:22:53 2014
Completed Surface Volume: 2D Area=656903.11657683 3D Area=677861.71322529 volume=55631646.074549
Succeeded at Mon May 12 16:22:53 2014 (Elapsed Time: 0.00 seconds)
Executing: Surfacevolume valden # BELOW 1754 1 0
```


Figure 7
[Click here to download high resolution image](#)

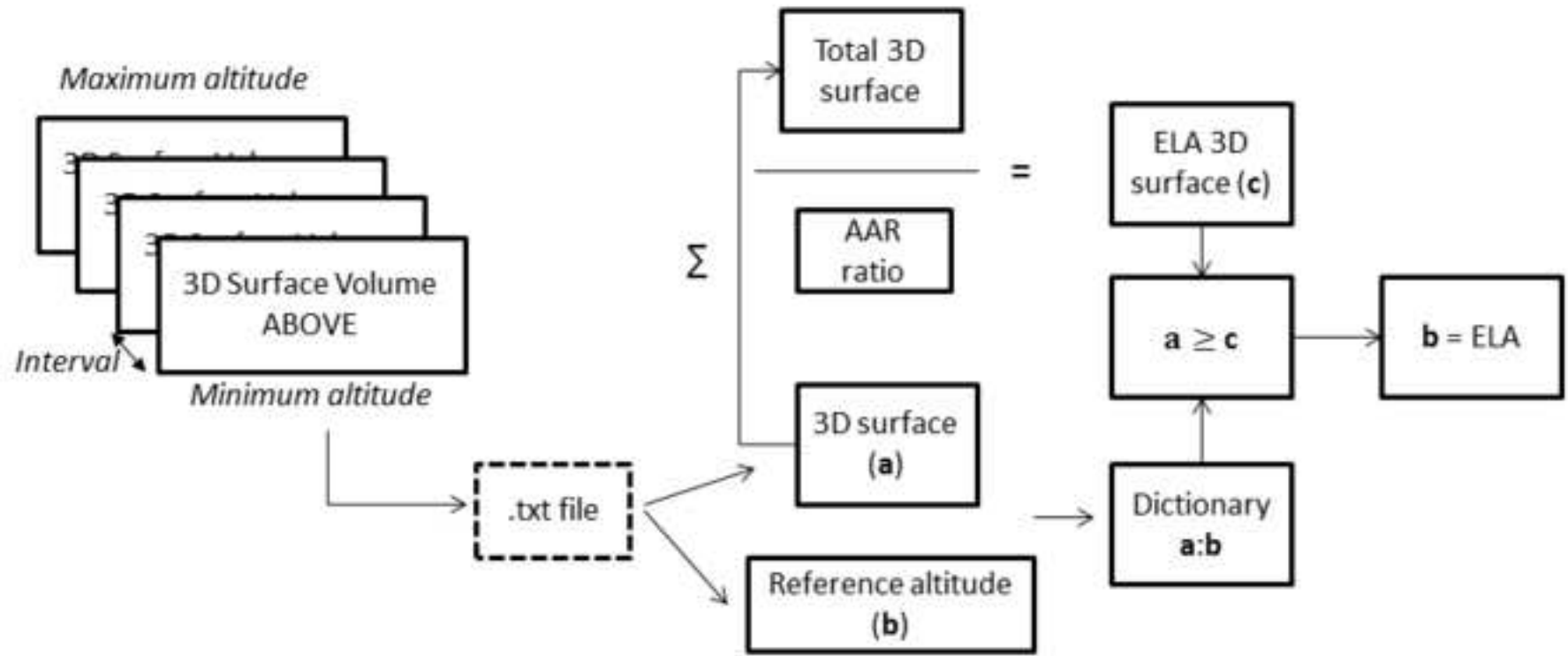


Figure 8
[Click here to download high resolution image](#)

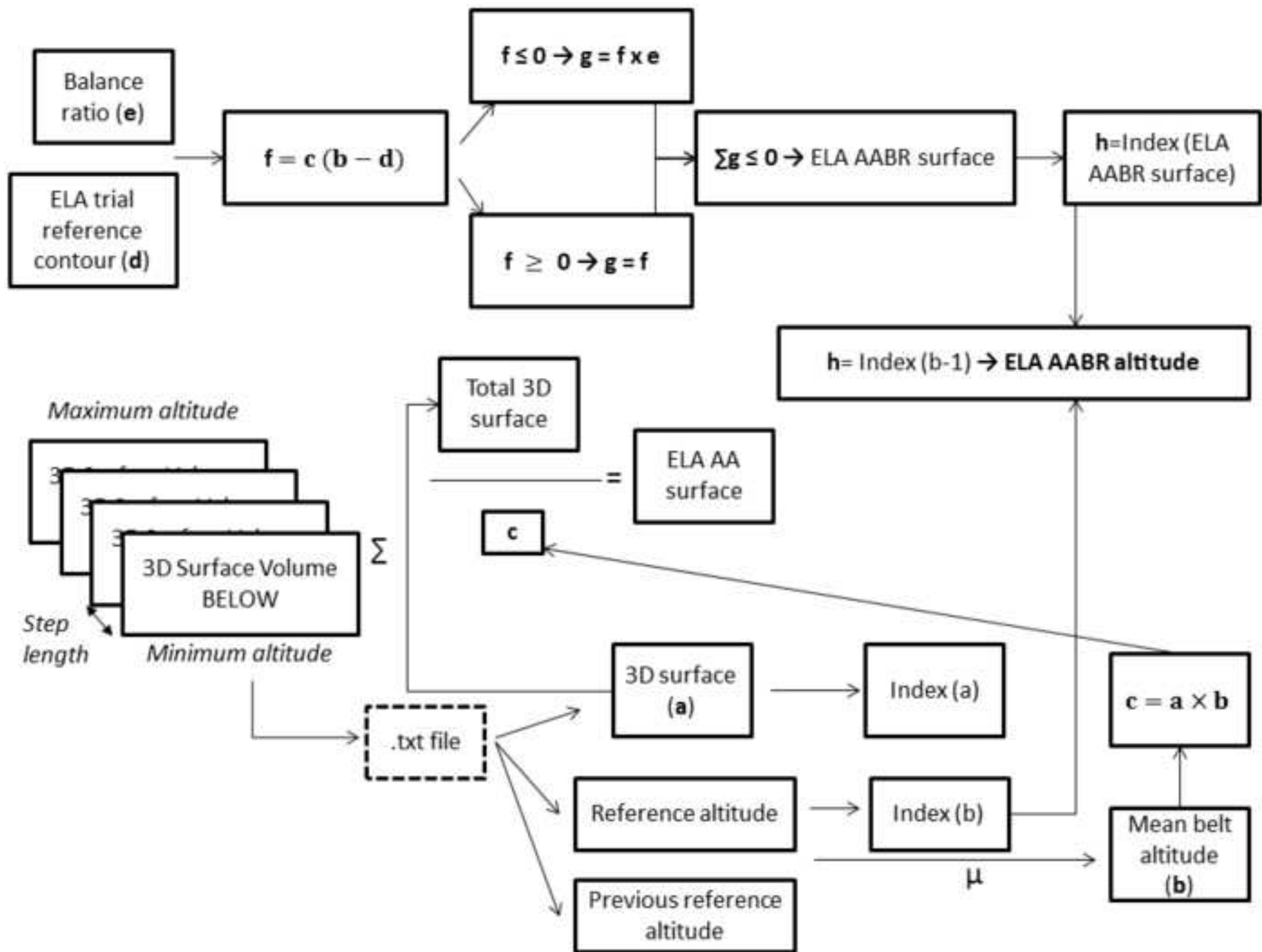


Table 1

Paper	Type of glacier (Location)	Ratio
Bakke and Nesje (2011)	Cirque and valley	0.6 ±0.05
Ignéczi and Nagy (2013)	Outlet	0.58
(Gross et al., 1978)	Cirque, valley and icefields (Alps)	0.67
Braithwaite and Müller (1980)	(Arctic, Alpine and Asian)	0.67
	(North America and Scandinavia)	0.5
	(Extremely high relief areas such as Andes or Himalayas)	<0.5
Clark et al. (1994)	Debris covered glaciers	0.2-0.1
Kern and Lazlo (2010)	0.1-1 km ² extension	0.44 ±0.07
	1-4 km ² extension	0.54±0.07
	Larger than 4 km ²	0.64 ± 0.04
	All glaciers (World Glacier Inventory)	0.559 ± 0.09
Leonard (1984), Hughes et al. (2010)	Ice caps	Up to 0.8

Table 1. AAR ratios suggested in the scientific literature.

Toolbox

[Click here to download Computer Code: ELA_calculation_OK_December.tbx](#)

AAR_script

[Click here to download Computer Code: AAR_un_DEM.py](#)

AABR_script

[Click here to download Computer Code: AABR_un_DEM.py](#)

AAR_AABR_several_ratios

[Click here to download Computer Code: AAR_AABR_AA_un_DEM_several_ratios.py](#)

AAR_AABR_several_ratios_several_DEMs

[Click here to download Computer Code: ELA_AABR_1.0_several_raster.py](#)